ISSN 1070-4272, Russian Journal of Applied Chemistry, 2020, Vol. 93, No. 3, pp. 325−332. © Pleiades Publishing, Ltd., 2020.
Russian Text © The Author(s), 2020, published in Zhurnal Prikladnoi Khimii, 2020, Vol. 93, No. 3, pp. 319−326.

PHYSICOCHEMICAL STUDIES OF SYSTEMS AND PROCESSES

Thermal Conductivity of Calcium Aluminate and Complex Vanadates of Garnet Structure

A. S. Tolkacheva[a,b,*], P. A. Popov[c], S. N. Shkerin[a,b], S. V. Naumov[d], P. D. Khavlyuk[e], A. A. Krugovykh[c], and S. V. Telegin[f]

[a] *Ural Federal University, Yekaterinburg, 620002 Russia*
[b] *Institute of High-Temperature Electrochemistry, Ural Branch, Russian Academy of Sciences, Yekaterinburg, 620137 Russia*
[c] *Petrovsky Bryansk State University, Bryansk, 241036 Russia*
[d] *Mikheev Institute of Metal Physics, Ural Branch, Russian Academy of Sciences, Yekaterinburg, 620137 Russia*
[e] *University of Information Technologies, Mechanics, and Optics, St. Petersburg, 197101 Russia*
[f] *Lobachevsky State University, Nizhny Novgorod, 603950 Russia*
**e-mail: a.s.tolkacheva@urfu.ru*

Received September 9, 2019; revised December 11, 2019; accepted December 14, 2019

Abstract—The thermal conductivity of materials with the nonstoichiometric garnet structure, namely, of calcium aluminate $Ca_{12}Al_{14}O_{33\pm\delta}$ (both single crystal and ceramic) and doped vanadates $Ca_5Mg_{4-x}M_x(VO_4)_6$ (M = Zn, Co; $0 \le x \le 4$), in the temperature interval 50–300 K was studied by the steady state comparative-longitudinal thermal flux method. The compositions $Ca_5Mg_{4-x}Zn_x(VO_4)_6$, x =1, 3, 4, were studied in the temperature interval 298–573 K by the dynamic method. The effect of the defective structure on the thermal conductivity of the materials was discussed. The thermal conductivity of the materials is ~2 W m^{-1} K^{-1} at room temperature and above.

Keywords: garnet, thermal conductivity, mayenite, vanadate, single crystal, $Ca_{12}Al_{14}O_{33}$

DOI: 10.1134/S1070427220030027

Garnets are complex oxides with the general formula $A_3B_2C_3O_{12}$, where cations A, B, and C are in sites with the coordination surrounding consisting of eight, six, and four oxygen atoms, respectively [1]. Such materials have a very rigid crystal lattice. For a long time, mutual substitutions were considered to be the most known defects in the garnet structure. Such defects consisted in partial occupation of a site corresponding to certain cations by cations of another kind. The problem of elimination of such defects stimulated the most extensive studies of such materials as $Y_3Al_2Al_3O_{12}$, $Gd_3Ga_2Ga_3O_{12}$, etc.

Active studies concerning the possibility of the existence of defective (nonstoichiometric) garnets were initiated quite recently. First and foremost, this problem is reflected in studies dealing with lithium-conducting electrolytes [2, 3]. The garnet $Li_7La_3Zr_2O_{12}$ is the only solid electrolyte stable in contact with lithium metal, though it is inferior to other materials in the conductivity.

The deviation of the stoichiometry from the base can be extremely large. For example, vanadates $Ca_5Mg_{4-x}Zn_x(VO_4)_6$ ($0 \le x \le 4$) in which every sixth site of cation A is vacant are known [4]. When a material contains no variable-valence cations, the occurrence of cationic vacancies is compensated by the appearance of the corresponding number of anionic vacancies. Thus, the total lattice defectiveness may be very high, but the "safety margin" of the garnet structure allows it to remain stable.

Calcium aluminate occupies a particular place among nonstoichiometric garnets. Its generalized composition is commonly described as $Ca_{12}Al_{14}O_{33\pm\delta}$ [5]. The natural form of this garnet is named mayenite; it corresponds to the garnet of the formula $Ca_{3-x}(Ca, Al)_{2-y}Al_3O_{12-z}$. Association of the defects around the largest of them, vacancy in A sublattice, occurring with decreasing temperature, leads to the appearance of structural features termed cages [6] (hollow spherical elements). The ap-

pearance of such structural features has also been reported for less defective garnets [7], but the structural feature of mayenite is that the cages contact with each other and form a subsystem. The cages are a factor stabilizing the electronic defects. For example, an oxygen vacancy inside a cage is a very stable trap state for an electron (F color center) and stabilizes it. Such materials were termed electrides [8]; they are being actively studied now [9–11]. An electron hole localized on the oxygen atom inside a cage [12] with the formation of a peroxide bond is stabilized similarly. Owing to this fact, low-temperature oxidation of silicon supports became possible [13]; it plays an important role in production of semiconductor devices. The presence of peroxy group in a mayenite-based catalyst prolongs its operation in a number of catalytic processes [14, 15].

The use of mayenite as a stable and available highly defective material for conservation of radioactive isotopes was suggested in 2019 [16]. Apparently, such material is resistant to radiation defects. High efficiency of using mayenite for the helium separation from a mixture of gases was demonstrated in [17]; thus, helium produced by α-decay will not give rise to mechanical stresses in the material. The problem of synthesis of a vacuum-tight ceramic for such filter has been successfully solved [18, 19].

Radioactive decay causes significant heating of the matrix material, which can lead to its degradation. However, the thermal conductivity of mayenite was not studied in detail. Only two papers can be mentioned. Kim et al. [20] compared the electride $C_{12}A_7$:e^- and mayenite in the oxidized state, $C_{12}A_7$:O^{2-}, at temperatures of up to 300 K. Rudradawong and Ruttanapun [21] studied the properties of mayenite reduced with carbon. We found no data on the thermal conductivity of calcium vanadates of the garnet structure. Calcium vanadates with the defectiveness similar to that of mayenite can also serve as a matrix for the storage or filtration of helium isotopes.

In connection with the above-discussed views on the defectiveness of such materials and prospects for their use, it seems interesting to study in more detail the thermal conductivity of calcium aluminates of the garnet structure and to determine the thermal conductivity of complex vanadates of the garnet structure.

EXPERIMENTAL

Calcium aluminate single crystal was grown by the zone melting method on a URN-2-3P installation of 5 kW power (assembled at National Research University MEI) using mayenite ceramic rods fabricated in advance as a semi-finished product, which prevents the formation of impurities in the crystals from the intermediate process steps. The rod size for the single crystal growth was 8 × 8 × 40 mm. The melting ceramic rod was arranged over the growing single crystal and was rotated independently of it in the direction opposite to the single crystal at a rate of 5–7 rpm under argon. The crystal growth rate was about 2 mm h^{-1}. A thin plate of the single crystal was cut perpendicularly to the growth axis defined as <210>. The structural analysis was performed by the Rietveld method using the FullProf program [22] (Fig. 1a). Single-phase samples of calcium aluminates (Fig. 1b) were synthesized by the sol–gel method with the subsequent heat treatment. To synthesize single-phase aluminate samples, we used $CaCO_3$ (chemically pure grade), $Al(NO_3)_3 \cdot 9H_2O$ (analytically pure grade), NH_4VO_3 (analytically pure grade), ethylene glycol, and nitric acid (ultrapure grade). The aqueous solution of the salts in the stoichiometric ratio was prepared with the addition of nitric acid. Ethylene glycol was introduced after complete dissolution of the starting components, and water was slowly evaporated to obtain a porous product, which was grounded, calcined at 700°C, and finally heat-treated at 1200°C for 48 h.

The following chemicals were used for the synthesis of vanadates: $CaCO_3$ (chemically pure grade), $MgCO_3$ (ultrapure grade), NH_4VO_3 (analytically pure grade), ZnO (chemically pure grade), formic acid HCOOH (pure grade, 99%), and citric acid $C_6H_8O_7 \cdot H_2O$ (chemically pure grade). Samples of the starting chemicals in the stoichiometric ratio were dissolved in distilled water, formic and citric acids were added, and the mixture was stirred on a heated magnetic stirrer for 2 h, after which it was evaporated to obtain a gel-like mass and finally dried in an oven at 120°C for 12 h; the dry powder was ground. The product was calcined at 600°C for 1 h. The pellets were compacted by uniaxial pressing. The final heat treatment was performed in alundum crucibles filled with the powder of the same composition as the pellet being fired. Up to 600°C, the samples were heated at a rate of 200 deg h^{-1} and then at a rate of 10 deg h^{-1} to a temperature from 800 to 970°C depending on the particular material. Finally, the samples were kept at the maximum temperature for 10 to 48 h in air. The single-phase composition of calcium vanadates was confirmed by comparing their diffraction patterns with the PDF #04-006-9985 card for $Ca_5Mg_4(VO_4)_6$ (Fig. 1c).

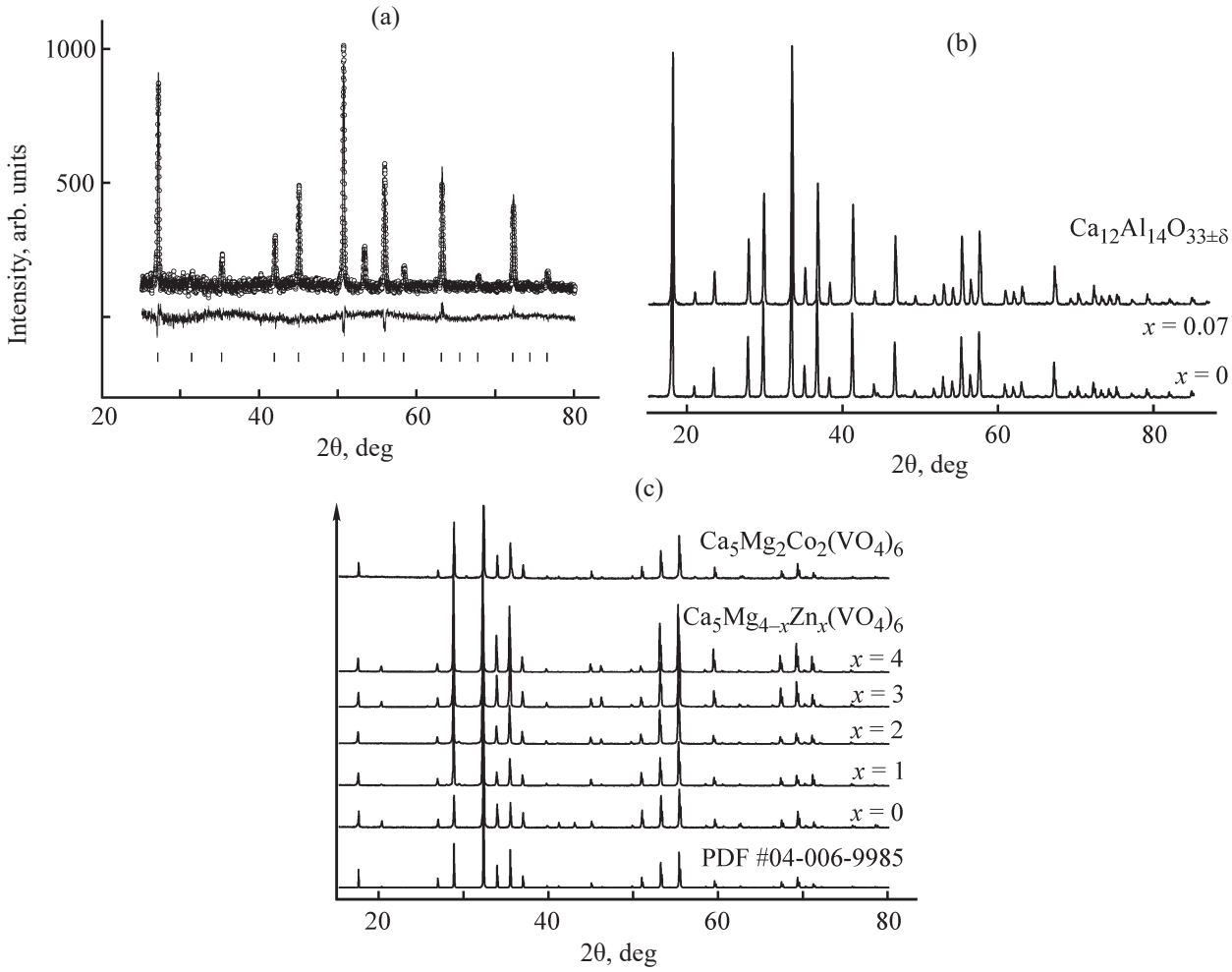

Fig. 1. Powder X-ray diffraction patterns (a) of the ground $Ca_{12}Al_{14}O_{33\pm\delta}$ single crystal and of ceramic samples of (b) mayenite and (c) calcium vanadates.

Certification of calcium vanadate and aluminate samples is described in more detail in [23, 24].

In the temperature interval 50–300 K, the thermal conductivity was measured by the Steady-state comparative-longitudinal thermal flux method with the error within ±6%. The measurement procedure and experimental apparatus are described in [25]. Three ceramic samples of the composition $Ca_5Mg_{4-x}M_x(VO_4)_6$ (x = 1, 3, 4) were studied in the interval 298–573 K by the dynamic method using an ITλ-400 meter with ±10% error.

RESULTS AND DISCUSSION

Thermal conductivity of calcium aluminates. The results of determining the thermal conductivity of calcium aluminate agree with the published data for the single crystal [20] and ceramic [21] (Fig. 2). Low thermal conductivity of mayenite $k(T)$ and weak temperature dependence of the thermal conductivity (Table 1), characteristic of media with significant disturbance of the long-range order, can be noted. A maximum of $k(T)$ in the region of $T \approx$ 50–90 K, smeared on the temperature scale, is observed for our ceramic and has been noted for the single crystal [20].

The presence of such maximum unambiguously demonstrates significant structural disordering of the material. It is known [26] that an increase in the defectiveness is accompanied by a decrease in the low-temperature maximum of $k(T)$ and by its shift toward higher temperatures. In this context, it can be expected that the defectiveness of the single crystal obtained in our study and of vanadium-doped aluminate ceramic (Fig. 2, curve *2*) is lower than that of the other samples. Near room temperature, the thermal conductivities

Apparent density, open porosity, and thermal conductivity of $Ca_{12-x}Al_{14-y}V_yO_{33\pm\delta}$ ($x = 0.7$; $y = 0.07$) and $Ca_5Mg_{4-x}M_x(VO_4)_6$ (M = Zn, Co; $0 \le x \le 4$)

Sample	Open porosity, %	Apparent density, g cm^{-3}	Thermal conductivity coefficient k, W m^{-1} K^{-1}	
			50 K	300 K
$Ca_{12}Al_{14}O_{33\pm\delta}$ single crystal	0	2.85	6.3	2.24
$Ca_{11.93}(Al_{14}V_{0.07})O_{33\pm\delta}$	0.1	2.61	4.28	2.12
$Ca_{12}Al_{14}O_{33\pm\delta}$ ceramic	0.1	2.60	2.56	2.04
$Ca_5Zn_4(VO_4)_6$	0.7	3.51	8.2	1.96
$Ca_5MgZn_3(VO_4)_6$	1.7	3.27	7.9	1.93
$Ca_5Mg_2Zn_2(VO_4)_6$	10	3.47	6.9	1.86
$Ca_5Mg_3Zn(VO_4)_6$	3	3.12	6.8	1.9
$Ca_5Mg_4(VO_4)_6$	3.8	3.18	9.0	2.2
$Ca_5Mg_2Co_2(VO_4)_6$	9	3.62	6.6	1.97

of the single-crystalline samples are virtually equal. The thermal conductivity of the ceramic samples is lower than that of the single-crystalline samples. This is primarily due to the finite porosity of the ceramic. The porosity of the ceramic is not indicated in [21]; however, for the samples in that study it was significant. It is known that preparation of a nonporous ceramic is a complex problem. The procedure for preparing a gastight ceramic based on mayenite has been protected by a patent [19].

Thermal conductivity of calcium vanadates. The low-temperature conductivity of vanadates is higher than that of aluminates (Fig. 3). Because near room temperature the thermal conductivities of vanadates and aluminates are close, the temperature dependences of $k(T)$ for these materials differ significantly.

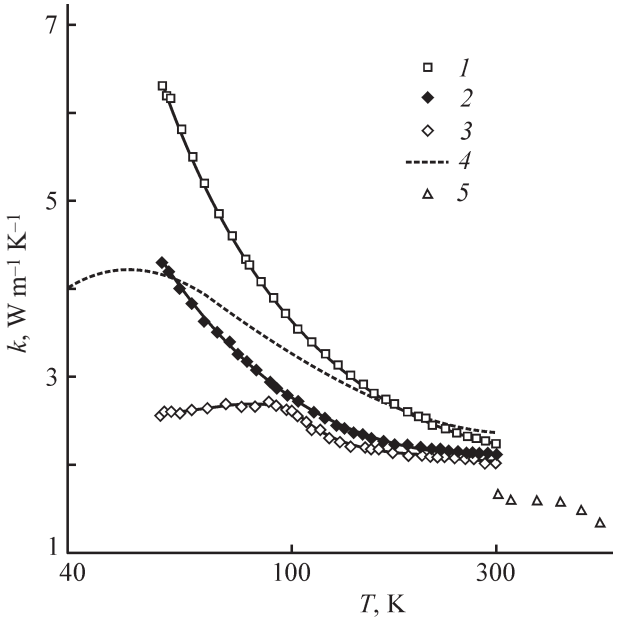

Fig. 2. Temperature dependence of the thermal conductivity of mayenite samples. Sample: (*1*) single crystal, (*2*) $Ca_{11.93}(Al_{14}V_{0.07})O_{33\pm\delta}$ ceramic, (*3*) $Ca_{12}Al_{14}O_{33\pm\delta}$ ceramic, (*4*) single crystal (data of [20]) and (*5*) ceramic (data of [21]).

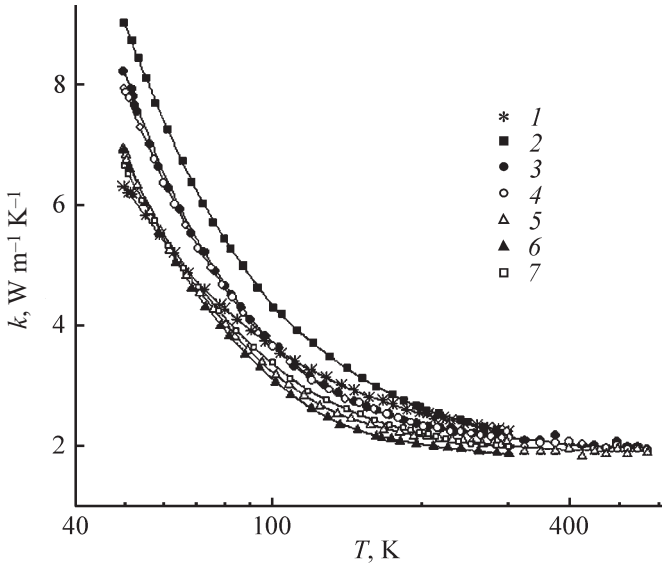

Fig. 3. Temperature dependence of the thermal conductivity of ceramic samples of vanadates in comparison with the mayenite single crystal. (*1*) $Ca_{12}Al_{14}O_{33\pm\delta}$ single crystal, (*2*) $Ca_5Mg_4(VO_4)_6$, (*3*) $Ca_5Zn_4(VO_4)_6$, (*4*) $Ca_5MgZn_3(VO_4)_6$, (*5*) $Ca_5Mg_3Zn(VO_4)_6$, (*6*) $Ca_5Mg_2Zn_2(VO_4)_6$, and (*7*) $Ca_5Mg_2Co_2(VO_4)_6$.

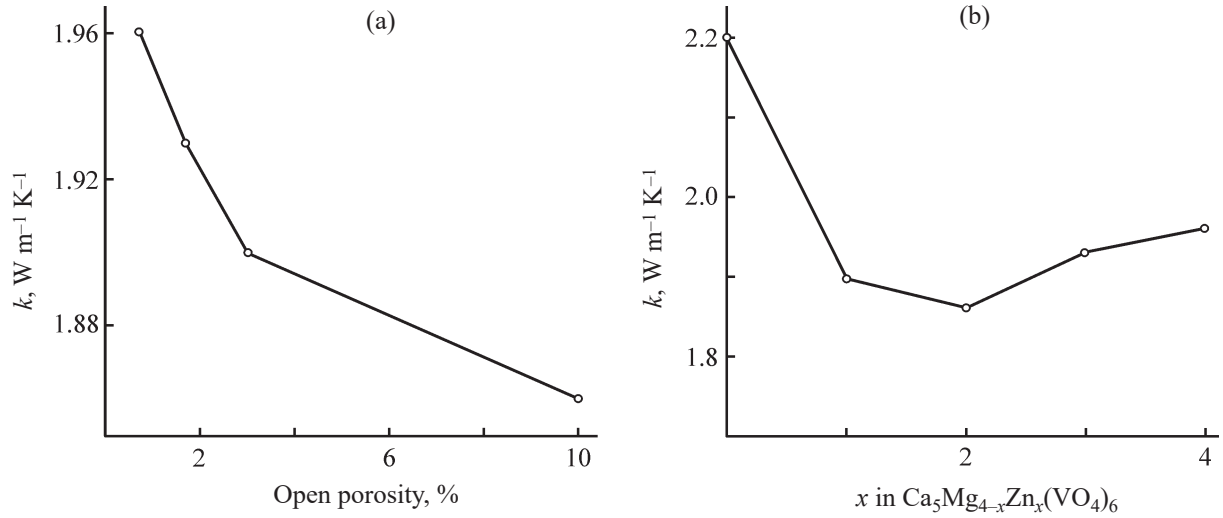

Fig. 4. Thermal conductivity at T = 300 K of the $Ca_5Mg_{4-x}Zn_x(VO_4)_6$ ceramic ($1 \le x \le 4$) as a function (a) of porosity and (b) of composition (including also data for $x = 0$).

As we saw for calcium aluminates (Fig. 2), the porosity of the ceramic is a critical parameter determining the thermal conductivity. Similarly, with an increase in the porosity of the $Ca_5Mg_{4-x}Zn_x(VO_4)_6$ ceramic ($1 \le x \le 4$), the thermal conductivity regularly decreases (Fig. 4). Thus, it can be noted that complication of the cationic composition upon partial isovalent replacement of magnesium by zinc and even cobalt is not accompanied by an appreciable decrease in the thermal conductivity. Apparently, this is caused by the initially intense phonon–defect scattering in ceramic vanadates of similar structural type. The only exception is the ceramic of the composition $Ca_5Mg_4(VO_4)_6$, which even at 3.8% porosity exhibits higher thermal conductivity compared to the other $Ca_5Mg_{4-x}Zn_x(VO_4)_6$ samples (Figs. 3, 4). This may be due to differences in the melting points T_m of these materials [24]. Within the framework of the phonon model of the heat transfer, the thermal conductivity k is determined by the heat capacity C of unit volume, mean velocity v of phonon propagation (sound), and mean phonon free path l [25]:

$$k = \frac{Cvl}{3}. \quad (1)$$

The characteristic temperature Θ related to T_m correlates with an increase in the heat capacity $C(T)$ in the examined temperature interval. Considerably higher melting point of $Ca_5Mg_4(VO_4)_6$ [24] is associated with higher strength of interatomic bonds, which in combination with relatively low true density determines relatively high mean phonon velocity.

Estimation of the mean free path of phonons in a mayenite single crystal. Because calcium aluminate single crystals are nonporous, the experimental values of the thermal conductivity allow estimation of the temperature dependence of the mean free path of phonons in the material. We found no experimental data on the heat capacity, except low-temperature values [11]; therefore, the temperature dependence of the molar heat capacity of $Ca_{12}Al_{14}O_{33\pm\delta}$ was calculated (Fig. 5) as an additive quantity from the values for its constituents, CaO and Al_2O_3. The calculation was performed in accordance with the Neumann–Kopp law using the formula

$$C_{Ca_{12}Al_{14}O_{33}} = 12C_{CaO} + 7C_{Al_2O_3}. \quad (2)$$

Extrapolation of the calculated heat capacities $C(T)$ to the melting point gives the value close to that determined by the Joule–Kopp law; for $Ca_{12}Al_{14}O_{33\pm\delta}$, it is $C \approx 1475$ J mol^{-1} K^{-1}.

The mean velocity of propagation of thermal phonons ν was estimated as follows. From the elastic constants c_{ij} [20], using the known relationships for the cubic system, we estimated the velocity of the longitudinal wave, ν_l, and of two transverse waves, ν_{S_1} and ν_{S_2}. The averaging was done in accordance with the formula

$$\frac{3}{v^3} = \frac{1}{v_i^3} + \frac{1}{v_{S_1}^3} + \frac{1}{v_{S_2}^3}.$$

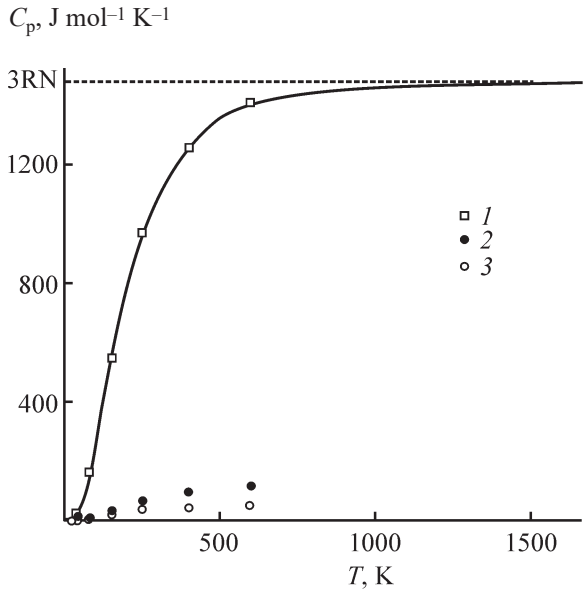

Fig. 5. Results of calculating the heat capacity of mayenite. (*1*) CaO, (*2*) Al_2O_3, and (*3*) $Ca_{12}Al_{14}O_{33\pm\delta}$.

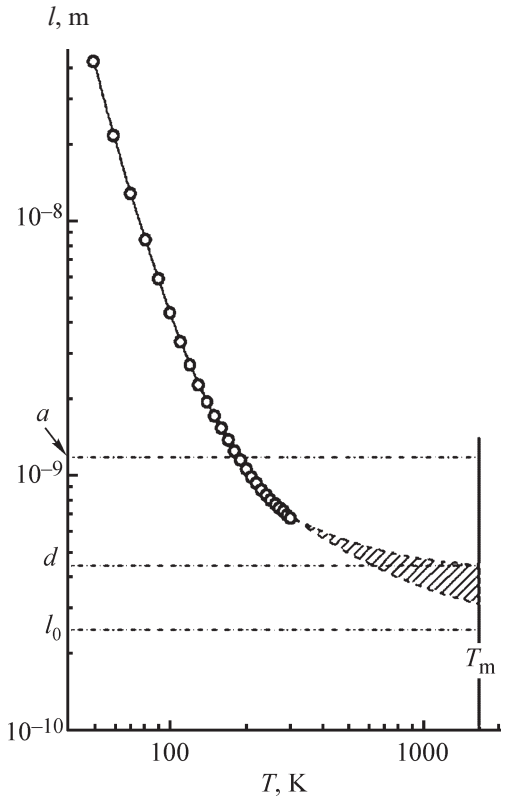

Fig. 6. Temperature dependence of the mean free path of phonons in the single-crystalline $Ca_{12}Al_{14}O_{33\pm\delta}$ sample. (*a*) Unit cell parameter of the garnet structure, (*d*) cage size, and (l_0) characteristic interstitial distance.

As we found, v varies with temperature insignificantly, from 4.91 km s^{-1} at T = 50 K to 4.86 km s^{-1} at T = 300 K.

The mean free path of phonons, $l(T)$, decreases with increasing temperature (Fig. 6) considerably more rapidly than the thermal conductivity $k(T)$ does. Whereas in the region of T = 300 K the temperature dependence of the thermal conductivity is described by the function $k = \text{Const} \times T^{-0.05}$, for the mean free path $l(T)$ the fitting dependence is stronger, $l = \text{Const} \times T^{-0.8}$, and is similar to dependences characteristic of single crystals with moderate phonon scattering intensity. In the region of T = 50 K, the corresponding functions can be presented in the form $k = \text{Const} \times T^{-0.7}$ and $l = \text{Const} \times T^{-3}$. Large slope of the $l(T)$ plot (Fig. 6) is apparently associated with the fact that the temperatures studied are far from the melting point of $Ca_{12}Al_{14}O_{33\pm\delta}$, which is as high as approximately 1650 K. The heat capacity at T = 300 K is less than 3/4 of the value determined by the Joule–Kopp law; therefore, in the region of room temperature the heat capacity continues to increase.

It should also be noted that the absolute value of the mean free path of phonons at the temperature increased to room temperature becomes lower than the unit cell parameter (a = 12 Å) of $Ca_{12}Al_{14}O_{33\pm\delta}$. At T = 300 K, the calculated value of l is 6.7 Å, which is very close to the value determined by Kim et al. [20] (7 Å). However, Kim et al. [20] used for the calculations the calorimetric data from [11], where the heat capacity below 5 K was measured, which casts doubts on the adequacy of the results they obtained.

Extrapolation of the calculated temperature dependence of the mean path length $l(T)$ to the region of the melting point gives the value between the unit cell parameter a and mean interstitial distance, l_0 = 2.45 Å in $Ca_{12}Al_{14}O_{33\pm\delta}$, and close to the cage cavity diameter d = 4.4 Å [27]. This fact confirms the conclusion on significant role of cages in limitation of the thermal conductivity of mayenite, made by Kim et al. [20].

The thermal conductivity of both calcium aluminates and calcium vanadates with the nonstoichiometric garnet structure at room temperature and above is of the order of 2 W m^{-1} K^{-1}. This is considerably lower than the thermal conductivity of defect-free single crystal of garnet $Y_3Al_5O_{12}$, equal to 11.2 W m^{-1} K^{-1}, but several times higher than the thermal conductivity of concrete or glass, i.e., of materials that are usually considered as host materials for storage of radioactive isotopes. It should be noted that in all the cases we deal with the phonon

mechanism of the heat transfer, because the materials do not have appreciable electronic conductivity. The materials studied are highly resistant to radiation defects and to the helium evolution in the bulk of the material due to α-decay; they are chemically durable and cheap.

CONCLUSION

At room temperature and above, the thermal conductivity of the vanadates $Ca_5Mg_{4-x}Zn_x(VO_4)_6$ ($0 \le x \le 4$) and $Ca_5Mg_2Co_2(VO_4)_6$ and of calcium aluminate $Ca_{12}Al_{14}O_{33\pm\delta}$ is of the order of 2 W m^{-1} K^{-1}. These materials have the structure of nonstoichiometric garnet and show promise for conservation of radioactive isotopes. The materials studied are highly resistant to radiation defects and to the helium evolution in the bulk of the material due to α-decay; they are chemically durable and cheap in production.

FUNDING

The study was performed using the equipment of the Center for Shared Use at the Institute of High-Temperature Electrochemistry, Ural Branch, Russian Academy of Sciences. The single crystal of mayenite was grown within the framework of Spin program of the Federal Agency of Scientific Organizations of the Russian Federation, no. AAAA-A18-118020290104-2. The study was financially supported in part by the Russian Foundation for Basic Research (project no. 17-03-01280_a).

CONFLICT OF INTEREST

The authors declare that they have no conflict of interest.

REFERENCES

1. Grew, E.S., Locock, A.J., Mills, S.J., Galuskina, I.O., Galuskin, E.V., and Hålenius, U., *Am. Miner.,* 2013, vol. 98, pp. 785–810. https://doi.org/10.2138/am.2013.4201
2. Murugan, R., Thangadurai, V., and Weppner, W., *Angew. Chem.,* 2007, vol. 46, pp. 7778–7781. https://doi.org/10.1002/anie.200701144
3. Wagner, R., Redhammer, G.J., Rettenwander, D., Tippelt, G., Welzl, A., Taibl, S., Fleig, J., Franz, A., Lottermoser, W., and Amthauer, G., *Chem. Mater.,* 2016, vol. 28, no. 16, pp. 5943–5951. https://doi.org/10.1021/acs.chemmater.6b02516
4. Mullerbuschbaum, H. and Vonpostel, M., *Z. Anorg. Allg. Chem.,* 1992, vol. 615, no. 9, pp. 101–103. https://doi.org/10.1002/zaac.19926150920
5. Armbruster, T. and Danisi, R.M., *Highlights in Mineralogical Crystallography,* Berlin: Walter de Gruyter, 2016.
6. Hosono, H. and Abe, Y., *Inorg. Chem.,* 1987, vol. 26, no. 8, pp. 1192–1195. https://doi.org/10.1021/ic00255a003
7. Grins, J., Istomin, S.Y., Svensson, G., Attfield, J.P., and Antipov, E., *J. Solid State Chem.,* 2005, vol. 178, no. 7, pp. 2197–2204. https://doi.org/10.1016/j.jssc.2005.04.029
8. Sushko, P.V., Shluger, A.L., Hayashi, K., Hirano, M., and Hosono, H., *Phys. Rev. Lett.,* 2003, vol. 91, no. 12, p. 126401. https://doi.org/10.1103/PhysRevLett.91.126401
9. Johnson, L.E., Sushko, P.V., Tomota, Y., and Hosono, H., *Proc. Natl. Acad. Sci. USA*, 2016, vol. 113, no. 36, pp. 10007–10012. https://doi.org/10.1073/pnas.1606891113
10. Kohama, Y., Kim, S.W., Tojo, T., Kawaji, H., Atake, T., Matsuishi, S., and Hosono, H., *Phys. Rev. B,* 2008, vol. 77, no. 9, p. 092505. https://doi.org/10.1103/PhysRevB.77.092505
11. Kohama, Y., Tojo, T., Kawaji, H., Atake, T., Matsuishi, S., and Hosono, H., *Chem. Phys. Lett.,* 2006, vol. 421, nos. 4–6, pp. 558–561. https://doi.org/10.1016/j.cplett.2006.02.016
12. Shkerin, S.N., Tolkacheva, A.S., Korzun, I.V., Plaksin, S.V., Vovkotrub, E.G., and Zabolotskaya, E.V., *J. Therm. Anal. Calorim.,* 2016, vol. 124, no. 3, pp. 1209–1216. https://doi.org/10.1007/s10973-016-5282-4
13. Nishioka, M., Nanjyo, H., Hamakawa, S., Kobayashi, K., Sato, K., Inoue, T., Mizukami, F., and Sadakata, M., *Solid State Ionics,* 2006, vol. 177, nos. 26–32, pp. 2235–2239. https://doi.org/10.1016/j.ssi.2006.08.007
14. Li, C.S., Hirabayashi, D., and Suzuki, K., *Appl. Catal. B: Environmental,* 2009, vol. 88, nos. 3–4, pp. 351–360. https://doi.org/10.1016/j.apcatb.2008.11.004
15. Mironova, E.Y., Ermilova, M.M., Orekhova, N.V., Tolkacheva, A.S., Shkerin, S.N., and Yaroslavtsev, A.B., *Nanotechnol. Russ.,* 2017, vol. 12, nos. 11–12, pp. 597–604. https://doi.org/10.1134/s1995078017060064
16. Kuganathan, N. and Chroneos, A., *Nanomaterials,* 2019, vol. 9, no. 6, p. E816. https://doi.org/10.3390/nano9060816
17. Tolkacheva, A.S., Shkerin, S.N., Kalinina, E.G., Filatov, I.E., and Safronov, A.P., *Russ. J. Appl. Chem.,*

2014, vol. 87, no. 4, pp. 536–538. https://doi.org/10.1134/s1070427214040235

18. Tolkacheva, A.S., Shkerin, S.N., Plaksin, S.V., Vovkotrub, E.G., Bulanin, K.M., Kochedykov, V.A., Ordinartsev, D.P., Gyrdasova, O.I., and Molchanova, N.G., *Russ. J. Appl. Chem.,* 2011, vol. 84, no. 6, pp. 907–911. https://doi.org/10.1134/s1070427211060012
19. Patent RU 2459781, Publ. 2012.
20. Kim, S.W., Tarumi, R., Iwasaki, H., Ohta, H., Hirano, M., and Hosono, H., *Phys. Rev. B,* 2009, vol. 80, no. 7, p. 075201. https://doi.org/10.1103/PhysRevB.80.075201
21. Rudradawong, C. and Ruttanapun, C., *Mater. Chem. Phys.,* 2019, vol. 226, pp. 296–301. https://doi.org/10.1016/j.matchemphys.2019.01.028
22. Rodriguez-Carvajal, J., *Physica B,* 1993, vol. 192, nos. 1–2, pp. 55–69. https://doi.org/10.1016/0921-4526(93)90108-I
23. Tolkacheva, A.S., Shkerin, S.N., Plaksin, S.V., Pankratov, A.A., and Moskalenko, N.I., *Refract. Ind. Ceram.,* 2019, vol. 60, no. 1, pp. 109–114. https://doi.org/10.1007/s11148-019-00318-w
24. Tolkacheva, A.S., Shkerin, S.N., Zemlyanoi, K.G., Reznitskikh, O.G., Pershina, S.V., and Khavlyuk, P.D., *J. Therm. Anal. Calorim.,* 2019, vol. 136, no. 3, pp. 1003–1009. https://doi.org/10.1007/s10973-018-7780-z
25. Popov, P.A., Sidorov, A.A., Kul'chenkov, E.A., Anishchenko, A.M., Avetisov, I.Ch., Sorokin, N.I., and Fedorov, P.P., *Ionics,* 2017, vol. 23, no. 1, pp. 233–239. https://doi.org/10.1007/s11581-016-1802-2
26. Berman, R., *Thermal Conduction in Solids,* Oxford: Clarendon, 1976, pp. 1–193.
27. Hosono, H., Hayashi, K., Kajihara, K., Sushko, P.V., and Shluger, A.L., *Solid State Ionics,* 2009, vol. 180, nos. 6–8, pp. 550–555. https://doi.org/10.1016/j.ssi.2008.10.015